06

Stages of the synthesis of carbon dots from citric acid and ethylenediamine: IR spectroscopy

© A.M. Vervald,[1] K.A. Laptinskiy,[2] M.Yu. Khmeleva,[1] T.A. Dolenko[1]

[1]Department of Physics, Lomonosov Moscow State University,
119991 Moscow, Russia
[2]Skobeltsyn Institute of Nuclear Physics, Lomonosov Moscow State University,
119991 Moscow, Russia
e-mail: alexey.vervald@physics.msu.ru

Received September 30, 2024
Revised September 30, 2024
Accepted September 30, 2024

Carbon dots synthesized by the hydrothermal method from citric acid and ethylenediamine have a luminescence quantum yield that significantly depends on the synthesis conditions and, under certain synthesis parameters, reaches more than 90%. To clarify the reasons for the dependence of the optical properties of carbon dots on the synthesis parameters, it is necessary to understand how their structure changes. For this purpose, in this paper we studied the relationship between structural changes and optical properties of carbon dots at different stages of their hydrothermal synthesis from a mixture of citric acid and ethylenediamine in a ratio of 1 : 1, achieved in 3 h of synthesis at a temperature varying from 80 to 200 °C with a step of 20 °C. As a result of the studies, the temperature boundaries of the stages of synthesis of carbon dots and changes in their structural and optical properties were determined: the beginning of the synthesis of luminescent structures; stage of active dehydration and carbonization of carbon dots with a concomitant increase in the number of both luminescent and non-luminescent chromophore structures; continuation of carbonization leading to the gradual destruction of luminescent structures. The change in chemical bonds in the reaction products during the synthesis process as the temperature increases is analyzed.

Keywords: photoluminescence, luminophores, spectroscopy, hydrothermal synthesis.

DOI: 10.61011/TP.2025.02.60816.280-24

Introduction

Carbon dots (CDs) first synthesized in 2004 [1] quickly attracted the interest when it became clear that these photoluminescent nanoparticles could be synthesized by a dozen of various methods from hundreds of various precursors: top−bottom from carbon macromaterials or bottom−top from almost any complex organic molecule mixture [2–6]. The source of CDs' photoluminescence may be surface states, defects in CD cores, individual molecular luminophores integrated into the CD core or the CD core itself due to the quantum confinement effect, if it has a crystalline structure [2–4,7,8]. Depending on the CD's structure, CD's luminescence spectrum can fall within a wide spectral range from ultraviolet to red region [2–4]. CDs' luminescence intensity depends on the ambient conditions in a different way: temperature, pH, presence of particular molecules or ions [9–13]. A wide variety of optical properties of CDs combined with non-toxicity, biocompatibility, chemical stability offers an opportunity of targeted selection for nanosensorics, optoelectronics and biomedicine applications [4,14,15].

CDs' luminescence quantum yield (LQY) is the most widely used parameter for comparison of various CDs with each other. While the LQY values for most of CDs fall within a range from units to several tens of percent points, LQY of some CDs may reach more than 90 % [6,16–18]. These are the LQY values that are achieved for CDs synthesized by the hydrothermal method from citric acid (CA) and ethylendiamine (EDA) [16–18]. However, such LQY is not always achieved, it depends on the main synthesis conditions — relation of the amount of precursors, nanoparticle synthesis temperature and time, with such dependencies being non-monotonic [18–21].

The latest results obtained from the analysis of morphology, luminescence excitation/emission maps and dialysis of CDs from CA and EDA [21–23] indicate that high CD LQY from CA and EDA is caused by molecular luminophores represented by CA and EDA copolymers. These luminophores are expected to be free or bound to the CDs' polymer scaffold. The authors of [21] consider citrazinic acid derivatives as such luminophores. Quantitative nuclear magnetic resonance (NMR) measurements indicate that an IPCA molecule (5-oxo-1,2,3,5-tetrahydroimidazo[1,2-a]pyridine-7-carboxylic acid) may serve as such luminophore [19,22]. The authors of [22] evaluated that the number of these molecules in CDs synthesized from CA and EDA through 360 W microwave radiation during 3 min was equal to 18 ± 2 wt.%.

The number of luminescent structures in CDs varies during the hydrothermal synthesis of CDs from CA and EDA [21]. Such variation is caused by chemical processes typical of hydrothermal synthesis of CDs: dehydration, polymerization, carbonization and passivation by organic molecules [24–28]. Our previous work [29] devoted to the study of properties of CDs synthesized from CA : EDA 1 : 2 (ratio of carboxyl and amino groups in this case is 3 : 4) at 140 °C during 0.5–6 h demonstrated the presence of several stages in the CD synthesis and found that longterm carbonization of CDs causes the destruction of their luminophores. However, the chemical processes taking place in other synthesis conditions may differ considerably, in particular, when there is excess in CA carboxyl groups over EDA amino groups. According to [29], IR absorption spectroscopy provides a large amount of information about CDs' transformation processes during hydrothermal synthesis in different conditions.

This study used the fluorescence spectroscopy, optical absorption and IR absorption spectroscopy methods to examine the luminescence and structural properties of CDs at different stages of hydrothermal nanoparticle synthesis from the EDA:CA 1 : 1 mixture during 3 h when the synthesis temperature varies from 80 to 200 °C in 20 °C steps.

1. Materials and methods

1.1. CD synthesis

CDs were synthesized by the hydrothermal method from CA (monohydrate, Ruskhim, AR grade) and EDA (made by EKOS-1, ACS grade) in bidistilled deionized water (conductivity 0.055 μS/cm, Millipore Milli-Qwater treatment system). For this, 10.53 g of CA was mixed with 3.35 mL of EDA and diluted with water to 500 mL (CA and EDA concentrations were 0.1 M, i.e. CA:EDA was equal to 1 : 1, the ratio of their carboxyl and amino groups was 3 : 2). Autoclaves with the prepared precursor mixture were held in the Sputnik (Russia) muffle furnace during 3 h at one of the temperatures within the variation range of 80–200 °C in 20 °C steps. Then, the autoclaves were removed from the furnace and cooled in air to room temperature. Thus synthesized CD samples were filtered through a membrane filter, mesh 0.22 μm.

1.2. CDs' study methods

pH of the CD solutions was measured using the Akvilon I-500 (Russia) pH meter, zeta potentials and hydrodynamic diameters were measured using the Malvern ZetaSizer Nano ZS instrument (UK).

IR absorption spectra of the concentrated CD gels were recorded using the Bruker INVENIO R (Germany) FTIR spectrometer in the attenuated total reflectance (ATR) mode. Gels were prepared by applying 15 μL CD aqueous solution to a 2×2 mm diamond crystal of the ATR module and drying in continuous ambient air flow during 10–15 min.

Photoluminescence spectra (PL) of the CDs' aqueous solutions were recorded using the Shimadzu RF-6000 (Japan) spectrofluorometer, absorbance spectra were recorded using the Shimadzu UV-1800 (Japan) spectrophotometer. PL and absorbance spectra of the synthesized CD samples were recorded after dilution with water to the absorbance at 345 nm equal to ~ 0.1. Such dilution was carried out to avoid the inner filter effect (IFE) [30] caused by absorption of both exciting and emitted CD light by the medium. For all degrees of dilution (DD), see the table.

The CDs' LQY was determined for the diluted solutions by the reference dye method [30] as follows

$$Q = Q_r \frac{OD_r}{OD} \frac{I}{I_r} \left(\frac{n}{n_r}\right)^2,$$

where Q is the carbon dots' LQY, OD is the optical density, I is the integral PL intensity, n is the refractive index of a medium, index „r“ indicates the equivalent parameters of the reference dye — quinine sulfate in aqueous solution of sulfuric acid (H_2SO_4 concentration was 0.05 M). All parameters were determined for $\lambda_{ex} = 345$ nm, 58 % was used as Q_r determined for a close excitation wavelength of 350 nm [30].

2. Characterization and photoluminescence properties of CDs

Aqueous suspensions of the synthesized CDs had pH values that decreased from 5.1 to 4.6 as the synthesis temperature varied from 80 to 120 °C, and then increase monotonously to 6.9 for CD 200 °C (see the table). pH approached 6.5 with dilution (see below). Note that within pH 5–7, photoluminescence of carbon nanoparticles, including CDs from CA and EDA, remains unchanged [11,12,31]. This means that the variations, obtained from the study and described below, of optical properties of CDs synthesized at different temperatures are not attributable to the pH variations of the CDs' environment.

Zeta potentials of the synthesized particles had dome-shaped distributions with FWHM of about 10 mV, the center of the distributions shifted gradually from 2mV to -5 mV as the synthesis temperature increased from 80 to 200 °C. Coarse nanoparticles with such zeta potentials are usually aggregated significantly [32,33], however, the CD synthesized from CA and EDA contained mainly a fraction with a hydrodynamic diameter of 0.7–1.3 nm and rare inclusions of $\sim$ 10 nm particles. Such size distribution is indicative of a colloidal stability mechanism caused by the stability of hydrated molecules, rather than by the zeta potential module.

The obtained photoluminescence excitation/emission maps of the aqueous solutions of all synthesized CDs appeared to be similar to each other (for examples, see Figure 1): they have two explicit maxima at $\lambda_{\mathrm{ex}}/\lambda_{\mathrm{em}} = 345/440$ and 242/440 nm/nm. An exception is the photoluminescence of the CD 80 °C sample solution, for which the luminescence emission maximum is at $\lambda_{\mathrm{em}} = 455$ nm. Difference in the photoluminescence intensity of the samples is also observed: if the maximum value for CD 80 °C is about

Parameters of the studied CD solutions: pH and dilution ratio (DDs) used for the samples, CDs’ photoluminescence properties at $\lambda_{\text{ex}} = 345$ nm: luminescence intensity measure and quantum yields of the synthesized CDs

Parameters	CDs synthesized at different temperatures						
Synthesis temperature	80 °C	100 °C	120 °C	140 °C	160 °C	180 °C	200 °C
pH of undiluted samples	5.1	4.9	4.6	4.8	5.3	6.0	6.9
DD	–	9.1	1001	3001	2801	834.3	601
$\lg(I_{\text{int}}$ [instrument un.]$\cdot$DD)	4.9	6.9	9.0	9.4	9.3	8.9	8.6
LQY*	15.8 %	76.0 %	88.6 %	77.0 %	66.8 %	65.9 %	61.7 %

Note. * statistical error of LQY measurement by the reference dye method is about 10% of the obtained value.

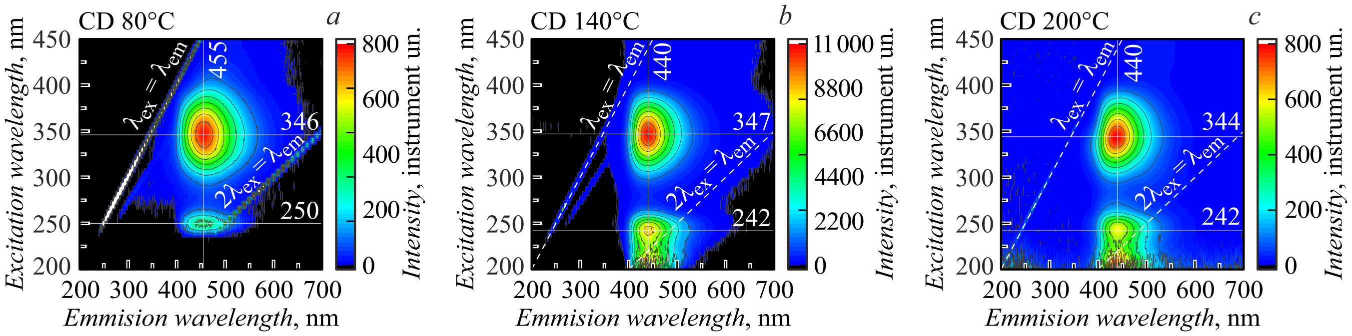

Figure 1. Photoluminescence excitation/emission maps of the aqueous solution: *a* — CD 80 °C, undiluted, *b* — CD 140 °C, 3001-fold diluted, *c* — CD 200 °C, 601-fold diluted.

800 instrument un., the maximum value for CD 140 °C is 14000 instrument un. This difference in radiation intensity of the CD samples turns out to be even bigger if the dilution ratio of synthesized CDs is taken into account (see below). Note also that CDs synthesized from CA : EDA 1 : 2 at 140 °C during 0.5–6 h, that were studied before [29], have almost the same luminescence map profiles with maxima at $\lambda_{\text{ex}}/\lambda_{\text{em}} = 350/440$ and 242/440 nm/nm. Similarity of luminescence maps between all CDs from CA : EDA 1 : 1 and 1 : 2 suggests that the structure of electronic transitions that are responsible for luminescence is almost the same, and the excess of the EDA NH_2 groups over the CA-COOH groups with CA : EDA 1 : 2 causes only the shift of absorption band maximum by 5 nm without changing the PL emission band maximum.

Two PL maxima in the luminescence map of the synthesized CDs at $\lambda_{\text{ex}}/\lambda_{\text{em}} = 345/440$ and 242/440 nm/nm (Figure 1) correspond to two highlighted CDs’ absorption bands at 242 nm and 345 nm (Figure 2, *a*) induced by the $\pi - \pi^*$ electronic transitions of C=C and/or C–N bonds and by the n–π^* transitions of C=O, C–N and/or C–OH bonds in sp^3domains, respectively [8,34]. Similarity of emission spectra with excitation at these two wavelengths, which is observed even when the radiation maximum for CD 80 °C is shifted by 15 nm, suggests that the observed two PL maxima are induced by the same CDs’ radiative center that has two different excitation paths (Figure 1).

The table shows the calculated LQY values with excitation of the main maximum of two luminescence maxima at 345 nm (Figure 2, *b*). Analysis of the corresponding absorbance spectra (Figure 2, *a*) shows that the maximum LQY value of 88.6 % for CD 120 °C corresponds to the optical absorption spectrum with the smallest background under the absorption band with the maximum at 345 nm, while the lowest LQY values, for example, LQY of 15.8 % for CD 80 °C, correspond to optical absorption spectra with a larger background under this absorption band (Figure 2, *a*). Considering the different dilution ratios of samples, this result suggests that, with the growth of the amount of absorbing synthesis products as the reaction temperature increases, the number of luminescent structures grows faster than the number of absorbing, but non-luminescent structures. At 120 °C, the maximum of this ratio is reached, absorption of luminescent structures becomes dominating.

Note that the absorption of various synthesized CDs at 345 nm differed by orders of magnitude, therefore different dilution degrees (DDs) of the sample solutions was necessary to achieve the absorbance at this wavelength ~ 0.1 to avoid IFE. With such dilution, luminescent particle concentration decreases proportionally and, consequently, the luminescence intensity decreases. To enable correct comparison of photoluminescence intensity of the synthesized CDs (remember that the same precursor solution was used for all CDs), their integral luminescence intensity I_{int} multiplied by DD shall be compared. Common logarithm

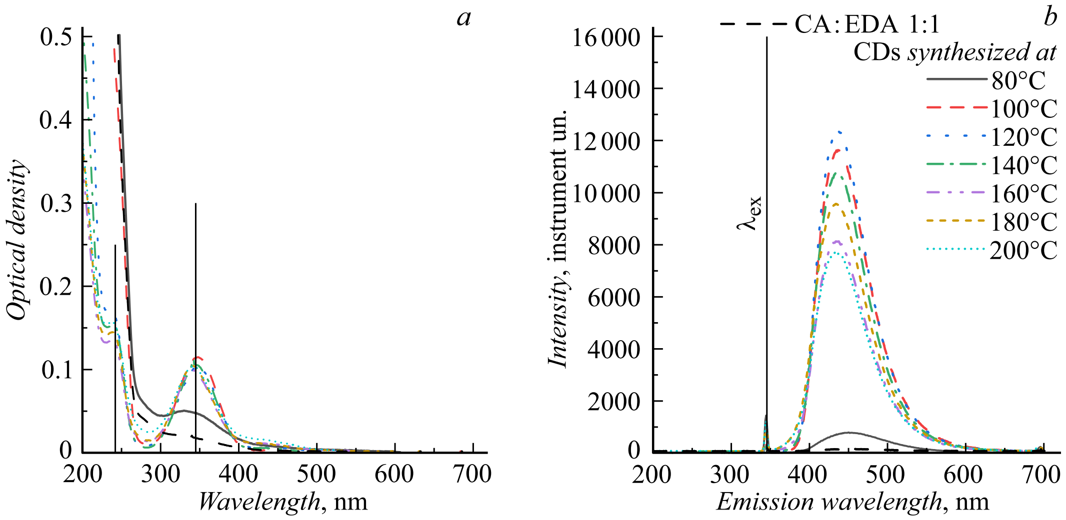

Figure 2. Optical density (a) and photoluminescence (*b*) spectra of the examined CD aqueous solutions.

of this quantity is shown in the table. It can be seen that the luminescence intensity for different undiluted CD solutions differs by a factor of 4.5. Taking into account the luminescence map profiles of all samples, this suggests that the number of synthesized luminescent structures in the samples also differs by a factor of 4 to 5.

3. IR spectroscopy of CD

IP absorption spectra of CDs obtained in the work (Figure 3) demonstrate a complex structure of the synthesized particles that varies depending on the synthesis temperature. All CDs' spectra show a wide absorption band at 2300−3800 cm^{-1} induced by stretching of −OH groups of surface-absorbed water particles (in the range of 3000−3800 cm^{-1}) and stretching of the functional group elements on the nanoparticle surface: carboxyl and hydroxyl groups (in the range of 2300−3300 cm^{-1}).

Two bands with maxima at 1700 and 1780 cm^{-1} correspond to C=O bond stretching in various environment [35]. The first of these bands in the spectra of the precursor and CD 80 °C mixture is closer to 1710 cm^{-1} and only at 120 °C shifts towards smaller wavenumbers to 1700 cm^{-1}. A band with a maximum at 1780 cm^{-1} becomes visible only at the nanoparticle synthesis temperature higher than 120 °C. Shift of the absorption band of C=O stretching towards lower frequencies is typical for lower degrees of carbon oxidation, i.e. the observed shift of this band by 10 cm^{-1} indicates that the -COOH carboxyl groups remaining from CA molecules that didn't react with EDA were destructed and replaced with $R_1-(\mathrm{C{=}O})-R_2$ carbonyl groups. This process is confirmed by the fact that at the synthesis temperature of 120 °C a band induced by stretching of C−O carboxyl groups with a maximum at 1186 cm^{-1} disappears (Figure 3). While a band with a maximum at 1780 cm^{-1} corresponds to stretching of C=O groups of conjugated anhydrides −(C=O)−O−(C=O)-. The shift and appearance of a new band are indicative of the precursor molecule polymerization stage through the carboxyl bond. However, for CDs with the synthesis temperature higher than 160 °C, decrease in the intensity of both of these bands is observed, C=O bands for them are destructed substantially. The presence and gradual transformation of carboxyl groups into CD synthesized from CA and EDA, which are observed in this work, are only typical for the case where the number of EDA amide groups is smaller than the number of CA carboxyl groups: when CA:EDA 1 : 2 (i.e. with the ratio of -COOH precursor groups to -NH$_2$ 3 : 4), C=O groups are no longer observed in the precursor mixture.

There is a deformation band of OH stretching at 1640 cm^{-1} (Figure 3). Starting from the synthesis temperature of 120 °C, a band with a maximum at 1646 cm^{-1} appears and grows. This band is induced by C=C bond stretching [36,37] and indicates that precursor carbonization grows. Note that this growth takes place simultaneously with the above-mentioned disintegration of carboxyl groups and remaining C=O bonds.

IR absorption spectra of CD also display bands of symmetric (1387 cm^{-1}) and asymmetric (1550 cm^{-1}) stretching of -NO$_2$ nitro groups. At the nanoparticle synthesis temperatures higher than 120 °C, absorption intensity of -NO$_2$ bands decreases, however, a band with a maximum at 1525 cm^{-1}, that is caused by stretching of -N=O nitroso groups, grows (Figure 3). The presence of nitro groups and nitroso groups in all CDs' and precursor mixture, the absence of these groups in molecules of individual precursors, and the absence of synthesis bands of -NH$_2$ amino groups and -CH$_2$- methylene groups of ethylendiamine (3400−3250 and 2800−3000 cm^{-1}) at the same time in the precursor mixture spectra, and then also in CDs' spectra are indicative of the active interaction between precursor molecules even before the start of synthesis. When the CDs' synthesis

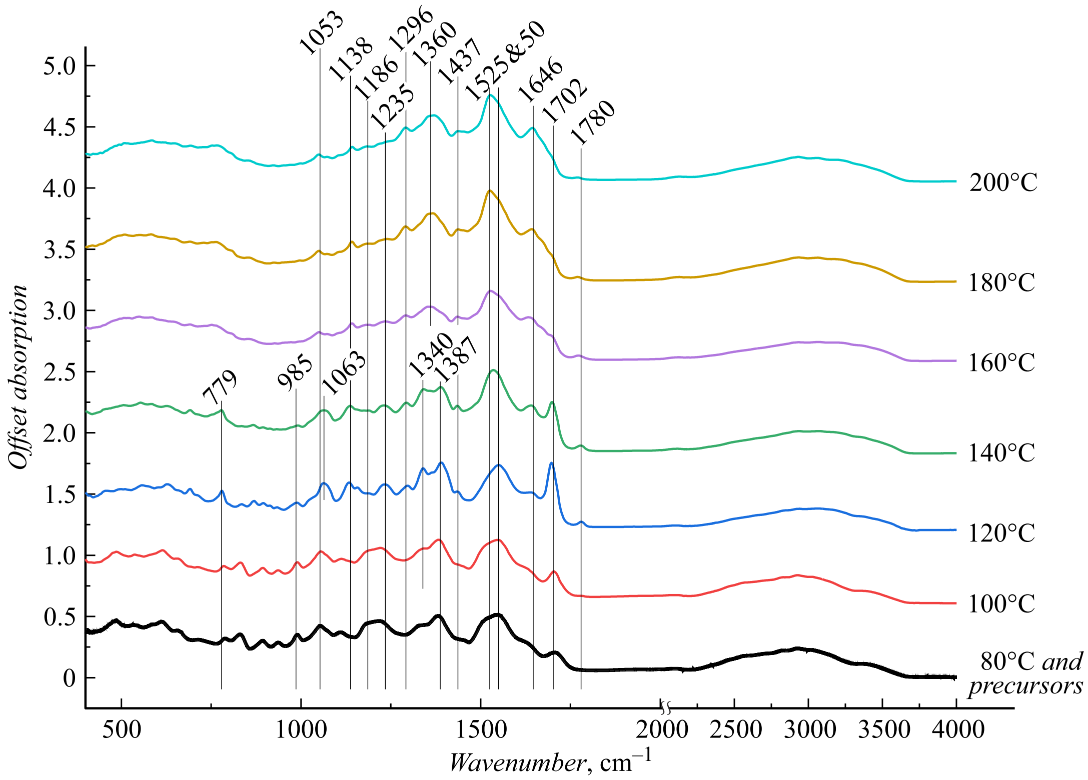

Figure 3. IR absorption spectra of the mixture of CD precursors and CDs synthesized at various synthesis temperatures.

temperature increases to 120 °C and higher, nitro groups, that were formed during mixing, are transformed into nitroso groups: dehydration process takes place.

Besides the bands listed above, the IR absorption spectra of CDs synthesized in this work from CA:EDA 1:1 during 3 h at various temperatures also have absorption bands with maxima at 1437, 1387, 1360, 1340, 1296, 1235, 1138, 1063, 1053, 985, 779 cm^{-1}, etc. (Figure 3). These bands are induced by stretching of C–N, N–H, C–H, C–O bonds and other groups, however, they cannot be interpreted accurately without knowing the structure of synthesized particles. At the same time, a common behavior of all these bands shall be noted: the mixture of precursors and CDs synthesized at 80 and 100 °C has a set of bands, spectra of CD synthesized at 120 and 140 °C have strongly pronounced new bands, and in spectra of CD synthesized at 160–200 °C, most of the maxima — both „old“, and new — are smeared. Pronounced narrow bands are indicative of a large amount of the same type of chemical bonds in the synthesized particle structure, while smearing of the bands is indicative of the versatility of these chemical bonds in the immediate environment.

The above-mentioned changes of CD chemical bond structure during the hydrothermal synthesis with temperature increasing from 80 to 200 °C, that are determined by the IR absorption spectra, correlate with the changes of photoluminescence properties of the synthesized CD (see the table). The mixture of precursor and CD synthesized at 80 °C don’t luminesce or luminesce weakly, which can be seen from the obtained luminescence intensity logarithm and LQY of the samples (see the table). As a result of the CDs’ synthesis at 100 °C, luminescence intensity in CDs grows by two orders of magnitude with respect to the luminescence intensity of CD 80 °C, which is also followed by a significant increase in LQY, however this intensity is still lower by two orders of magnitude than the maximum value (see the table). IR absorption spectra of precursors and CDs synthesized at 80 and 100 °C are similar to each other: synthesis reaction of luminescent structures at such temperatures flows slowly and fails to change a large fraction of intermolecular bonds during 3 h. During the CDs’ synthesis at 120 and 140 °C, dehydration, carbonization and polymerization processes take place: nitro groups are transformed into nitroso groups, C=C bonds are formed, carboxyl groups „loose“ –OH bonds and „close“ on carbon or on the identical groups of other molecules to form conjugated anhydrides. These formed structures have the most pronounced similarity of chemical bonds among all synthesized CDs. At 120 °C, 100 times as many luminescent structures are synthesized than at 100 °C, thus, providing the highest LQY among the studied CDs — the largest ratio of luminescent fraction to just absorbing fraction. Whereas the synthesis at 140 °C causes the continued synthesis of the luminescent fraction — its amount grows by an additional factor of 2.5 — however, the amount of the absorbing, but non-luminescent fraction also increases: LQY decreases (see the tables). At the CDs' synthes is temperature from 160 to 200 °C during the synthes is time of 3 h, more active CD carbonization takes place and is followed by destruction of C=O bonds and increase in the versatility of CDs' bonds environment. Analysis of the luminescence properties of CDs suggests that a part of luminescent CDs' structures is destructed at this synthesis stage.

Conclusion

The study investigated the correlation of structural changes and optical properties of CDs at various stages of hydrothermal synthesis from 1 : 1 CA and EDA mixture during 3 h in a wide temperature variation range from 80 to 200 °C. Information about structural features of CDs was obtained by the IR absorption spectroscopy method.

It was found that:

– when mixing EDA and CA precursors at room temperature, EDA nitrogen atoms react with CA carboxyl groups to form nitro groups and nitroso groups;

– during the 3-hour CD synthesis process at temperatures from 80 to 100 °C , transformations of chemical bonds that are visible in the IR absorption spectra are not observed in the reaction products. However, luminescent structures with luminescence maxima at $\lambda_{\text{ex}}/\lambda_{\text{em}} = 345/440$ and 242/440 nm/nm start to be synthesized and their number grows as the temperature increases, thus, causing the growth of LQY from 15.8 % to 76 %;

– at higher temperatures from 120 to 160 °C during 3 h of synthesis, considerable changes occur in the CD structure: -NO_2 groups are replaced with -N=O groups, C=C bonds and conjugated anhydrides are formed. These changes are indicative of the dehydration, carbonization and polymerization processes in the reaction medium. These are the synthesis stages, at which the highest PL intensity and CDs' LQY are observed, i.e. a significant growth of luminescent structures.

– according to the IR absorption spectroscopy data, carbonization becomes quite active at even higher synthesis temperatures from 160 to200 °C. It is followed by destruction of C=O bonds and significant increase in the versatility of CDs' bonds in the environment. Whereas CD LQY and luminescence intensity decrease, i.e. luminescent structures of CDs are destructed at this stage.

The established correlation between structural changes and optical properties of CDs at various stages of hydrothermal synthesis from the CA and EDA mixture makes it possible to choose the best synthesis conditions for successful solution of certain problems not only for the CD synthesis with pre-defined luminescence properties, but also with pre-defined chemical bonds. Thus, the work demonstrates the importance of IR absorption spectra measurements of the synthesized CDs for evaluation of the changes in the composition of CDs' surface groups, uniformity or versatility of their chemical bonds, apart from the photoluminescence property measurements.

Acknowledgments

Some experimental data used in this work was obtained using a Fourier transform IR spectrometer that was purchased under the Development Program of Moscow State University (agreement No. 65 as of October 04, 2021).

Funding

The study was supported by the Russian Science Foundation grant no. 23-72-01042, https://rscf.ru/en/project/23-72-01042/.

Conflict of interest

The authors declare no conflict of interest.

References

[1] X. Xu, R. Ray, Y. Gu, H.J. Ploehn, L. Gearheart, K. Raker, W.A. Scrivens. J. Am. Chem. Soc., **126**, 12736 (2004). DOI: 10.1021/ja040082h

[2] S. Zhu, Y. Song, X. Zhao, J. Shao, J. Zhang, B. Yang. Nano Res., **8**, 355 (2015). DOI: 10.1007/s12274-014-0644-3

[3] C. Xia, S. Zhu, T. Feng, M. Yang, B. Yang. Adv. Sci., **6**, 1901316 (2019). DOI: 10.1002/advs.201901316

[4] D. Ozyurt, M.A. Kobaisi, R.K. Hocking, B. Fox. Carbon Trends, **12**, 100276 (2023). DOI: 10.1016/j.cartre.2023.100276

[5] H. Liu, X. Zhong, Q. Pan, Y. Zhang, W. Deng, G. Zou, H. Hou, X. Ji. Coord. Chem. Rev., **498**, 215468 (2024). DOI: 10.1016/j.ccr.2023.215468

[6] N.A. Nazibudin, M.F. Zainuddin, C.A.C. Abdullah. J. Adv. Res. Fluid Mech. Therm. Sci., **101**, 192 (2023). DOI: 10.37934/arfmts.101.1.192206

[7] M.A. Sk, A. Ananthanarayanan, L. Huang, K.H. Lim, P. Chen. J. Mater. Chem. C, **2**, 6954 (2014). DOI: 10.1039/C4TC01191K

[8] Y. Zhang, R. Yuan, M. He, G. Hu, J. Jiang, T. Xu, L. Zhou, W. Chen, W. Xiang, X. Liang. Nanoscale, **9**, 17849 (2017). DOI: 10.1039/C7NR05363K

[9] H. Zhang, J. You, J. Wang, X. Dong, R. Guan, D. Cao. Dyes Pigm., **173**, 107950 (2020). DOI: 10.1016/j.dyepig.2019.107950

[10] X.-J. Xu, S. Ge, D.-Q. Li, Z.-Q. Xu, E.-J. Wang, S.-M. Wang. Chin. J. Anal. Chem., **50**, 103 (2022). DOI: 10.1016/j.cjac.2021.09.005

[11] A.M. Vervald, K.A. Laptinskiy, G.N. Chugreeva, S.A. Burikov, T.A. Dolenko. J. Phys. Chem. C, **127**, 21617 (2023). DOI: 10.1021/acs.jpcc.3c05231

[12] M.Yu. Khmeleva, K.A. Laptinskiy, T.A. Dolenko. Opt. i spektr., **131**, 797 (2023) (in Russian). DOI: 10.21883/OS.2023.06.55913.104-23, [M.Yu. Khmeleva, K.A. Laptinskiy, T.A. Dolenko. Opt. Spectr., **6**, 752 (2023). DOI: 10.61011/EOS.2023.06.56662.104-23]

[13] A.M. Vervald, A.D. Salekhov, T.A. Dolenko. J. Sib. Fed. Univ. Math. Phys., **15** (6), 710 (2022). DOI: 10.17516/1997-1397-2022-15-6-710-717

[14] M. Jorns, D. Pappas. Nanomater., **11**, 1448 (2021). DOI: 10.3390/nano11061448

[15] B.D. Mansuriya, Z. Altintas. Nanomater., **11**, 2525 (2021). DOI: 10.3390/nano11102525

[16] N.A.S. Omar, Y.W. Fen, R. Irmawati, H.S. Hashim, N.S.M. Ramdzan, N.I.M. Fauzi. Nanomater., **12**, 2365 (2022). DOI: 10.3390/nano12142365

[17] J. Ren, L. Malfatti, P. Innocenzi. C, **7**, 2 (2020). DOI: 10.3390/c7010002

[18] D. Qu, M. Zheng, L. Zhang, H. Zhao, Z. Xie, X. Jing, R.E. Haddad, H. Fan, Z. Sun. Sci. Rep., **4**, 5294 (2014). DOI: 10.1038/srep05294

[19] Y. Song, S. Zhu, S. Zhang, Y. Fu, L. Wang, X. Zhao, B. Yang. J. Mater. Chem. C, **3**, 5976 (2015). DOI: 10.1039/C5TC00813A

[20] S. Zhu, Q. Meng, L. Wang, J. Zhang, Y. Song, H. Jin, K. Zhang, H. Sun, H. Wang, B. Yang. Angew. Chem. Int. Ed., **52**, 3953 (2013). DOI: 10.1002/anie.201300519

[21] M. Zhang, X. Long, Y. Ma, S. Wu. Opt. Mater., **135**, 113311 (2023). DOI: 10.1016/j.optmat.2022.113311

[22] P. Duan, B. Zhi, L. Coburn, C.L. Haynes, K. Schmidt-Rohr. Magn. Reson. Chem., **58**, 1130 (2020). DOI: 10.1002/mrc.4985

[23] J. Manioudakis, F. Victoria, C.A. Thompson, L. Brown, M. Movsum, R. Lucifero, R. Naccache. J. Mater. Chem. C, **7**, 853 (2019). DOI: 10.1039/C8TC04821E

[24] S. Rodríguez-Varillas, T. Fontanil, Á.J. Obaya, A. Fernández-González, C. Murru, R. Badía-Laíño. Appl. Sci., **12**, 773 (2022). DOI: 10.3390/app12020773

[25] N. Papaioannou, M.-M. Titirici, A. Sapelkin. ACS Omega, **4**, 21658 (2019). DOI: 10.1021/acsomega.9b01798

[26] S. Tao, T. Feng, C. Zheng, S. Zhu, B. Yang, J. Phys. Chem. Lett., **10**, 5182 (2019). DOI: 10.1021/acs.jpclett.9b01384

[27] Y. Hu, J. Yang, J. Tian, J.-S. Yu. J. Mater. Chem. B, **3**, 5608 (2015). DOI: 10.1039/C5TB01005E

[28] L. Ai, Y. Yang, B. Wang, J. Chang, Z. Tang, B. Yang, S. Lu. Sci. Bull., **66**, 839 (2021). DOI: 10.1016/j.scib.2020.12.015

[29] A.M. Vervald, K.A. Lapinsky, M.Yu. Khmelyova, T.A. Dolenko Opt. i spectrosc., **132** (3), 11 (2024) (in Russian). DOI: 10.61011/OS.2024.03.58140.24-24

[30] J.R. Lakowicz. ed. *Principles of Fluorescence Spectroscopy* (Springer, US, 2006), DOI: 10.1007/978-0-387-46312-4

[31] A.M. Vervald, A.V. Lachko, O.S. Kudryavtsev, O.A. Shenderova, S.V. Kuznetsov, I.I. Vlasov, T.A. Dolenko. J. Phys. Chem. C, **125**, 18247 (2021). DOI: 10.1021/acs.jpcc.1c03331

[32] D.J. Pochapski, C. Carvalho dos Santos, G.W. Leite, S.H. Pulcinelli, C.V. Santilli. Langmuir, **37**, 13379 (2021). DOI: 10.1021/acs.langmuir.1c02056

[33] T. Fiuza, G. Gomide, A.F.C. Campos, F. Messina. J. Depeyrot, C, **5**, 74 (2019). DOI: 10.3390/c5040074

[34] A.N. Emam, S.A. Loutfy, A.A. Mostafa, H. Awad, M.B. Mohamed. RSC Adv., **7**, 23502 (2017). DOI: 10.1039/C7RA01423F

[35] G. Socrates. *Infrared and Raman Characteristic Group Frequencies: Tables and Charts.* 3rd ed. (University of West London, Middlesex, UK., 2001)

[36] R. Ludmerczki, S. Mura, C.M. Carbonaro, I.M. Mandity, M. Carraro, N. Senes, S. Garroni, G. Granozzi, L. Calvillo, S. Marras, L. Malfatti, P. Innocenzi. Chem. Eur. J., **25**, 11963 (2019). DOI: 10.1002/chem.201902497

[37] B.C. Smith. Spectroscopy, **31** (11), 28 (2016).

Translated by E.Ilinskaya